



HAL
open science

Assessment of an e-nose performance for the detection of COVID-19 specific biomarkers

Christelle Ghazaly, Krystyna Biletska, Etienne Thevenot, Philippe Devillier, Emmanuel Naline, Stanislas Grassin-Delyle, Emmanuel Scorsone

► **To cite this version:**

Christelle Ghazaly, Krystyna Biletska, Etienne Thevenot, Philippe Devillier, Emmanuel Naline, et al.. Assessment of an e-nose performance for the detection of COVID-19 specific biomarkers. *Journal of Breath Research*, 2023, 17 (2), pp.026006. 10.1088/1752-7163/acb9b2 . cea-04080762

HAL Id: cea-04080762

<https://cea.hal.science/cea-04080762>

Submitted on 27 Apr 2023

HAL is a multi-disciplinary open access archive for the deposit and dissemination of scientific research documents, whether they are published or not. The documents may come from teaching and research institutions in France or abroad, or from public or private research centers.

L'archive ouverte pluridisciplinaire **HAL**, est destinée au dépôt et à la diffusion de documents scientifiques de niveau recherche, publiés ou non, émanant des établissements d'enseignement et de recherche français ou étrangers, des laboratoires publics ou privés.

Assessment of an e-nose performance for the detection of COVID-19 specific biomarkers

Christelle GHAZALY^a, Krystyna BILETSKA^a, Etienne A. THEVENOT^b, Philippe DEVILLIER^{c,d}, Emmanuel NALINE^{c,d}, Stanislas GRASSIN-DELYLE^{c,e}, Emmanuel SCORSONE^{a*}

^a Université Paris-Saclay, CEA, LIST, F-91120 Palaiseau, France

^b Département Médicaments et Technologies pour la Santé (DMTS), Université Paris-Saclay, CEA, INRAE, MetaboHUB, 91191 Gif-sur-Yvette, France

^c Hôpital Foch, Exhalomics, Département des maladies des voies respiratoires, Suresnes, France

^d VIM Suresnes, UMR-0892, Université Paris-Saclay, UVSQ Suresnes, France.

^e Infection et inflammation, Département de Biotechnologie de la Santé, Université Paris-Saclay, UVSQ, INSERM, Montigny le Bretonneux, France

E-mail: Emmanuel.scorsone@cea.fr

Received xxxxxx

Accepted for publication xxxxxx

Published xxxxxx

Abstract

Early, rapid and non-invasive diagnosis of Severe Acute Respiratory Syndrome CoronaVirus 2 (SARS-CoV-2) infection is needed for the prevention and control of coronavirus disease 2019 (COVID-19). COVID-19 mainly affects the respiratory tract and lungs. Therefore, analysis of exhaled breath could be an alternative scalable method for reliable SARS-CoV-2 screening. In the current study, an experimental protocol using an electronic-nose ("e-nose") for attempting to identify a specific respiratory imprint in COVID-19 patients was optimized. Thus the analytical performances of the Cyranose[®], a commercial e-nose device, were characterized under various controlled conditions. In addition, the effect of various experimental conditions on its sensor array response was assessed, including relative humidity, sampling time and flow rate, aiming to select the optimal parameters. A statistical data analysis was applied to e-nose sensor response using common statistical analysis algorithms in an attempt to demonstrate the possibility to detect the presence of low concentrations of spiked acetone and nonanal in the breath samples of a healthy volunteer. Cyranose[®] reveals a possible detection of low concentrations of these two compounds, in particular of 25 ppm nonanal, a possible marker of SARS-CoV-2 in the breath.

Keywords: COVID-19, SARS-COV-2, breath-analysis, electronic-nose, Volatile Organic Compounds, nonanal.

1. Introduction

Severe Acute Respiratory Syndrome CoronaVirus 2 (SARS-CoV-2), caused more than 600 million infections and 6 million deaths since it appeared in December 2019 [1]. Rapid detection of SARS-CoV-2 infection remains a necessity for the prevention and control of the pandemic. The standard diagnostic method is based on viral genome detection in nasopharyngeal or oropharyngeal samples with Polymerase Chain Reaction (PCR). PCR testing is based on an invasive, costly procedure and requires qualified personnel. Other tests used for identifying COVID-19 infection include Rapid Antigen Detection Tests (RADTs)

and chest scans [2]. RADTs are less sensitive than PCR test and could be usefully complemented by non-invasive, fast, reliable, cheap methods for screening individuals in busy areas (e.g. airports and, railway stations) or remote areas.

COVID-19 mainly affects the respiratory tract and lungs [3]. Therefore, analysis of exhaled breath could be a non-invasive alternative that could be scaled up for fast and reliable SARS-CoV-2 screening. Exhaled breath consists of a mixture of gases, water vapor and Volatile Organic Compounds (VOCs), whose abundance, specificity and nature can vary from a healthy to an ill individual [4]. Breath analysis has previously been used for detecting VOCs signatures resulting from various infections or chronic diseases [5]. Here both temperature and relative humidity are

two of the most important variables, that influence on the reproducibility and reliability of measurements, that have been studied in previous research where the correlation of these factors with clinical and environmental parameters was studied [6].

Many techniques are used for breath analysis, including mass spectrometry and sensor-based technologies [7,8]. Different mass spectrometry or ion mobility spectrometry methods were applied to identify a breathprint of COVID-19. These studies suggested that VOCs from different families including alcohols, aldehydes, ketones, or alkenes may distinguish individuals with or without COVID-19. Commonly reported VOCs include nonanal, which was suggested to be representative SARS-CoV-2-related VOC biomarkers in studies in adults and children [9,10].

Besides, electronic noses "e-noses" are handheld, sensitive, selective, low-cost and rapid devices that are used for breath analysis. These devices consist mainly of air sampling in the headspace, an integrated sensor array based on various optical, gravimetric, electrochemical or capacitive transduction systems and a signal-processing algorithm. E-noses rely on the interaction between the sensors with the VOCs present in the sampled air, inducing a change in the physical properties of the sensors and generating a typical signal representative of the VOCs present in the tested sample [11]. There are potential applications of e-noses in the field of environmental monitoring, the foodstuffs and beverage quality control, in odor control in the aircraft and automobile and in the diagnosis or monitoring diseases according to specific breathprints [12]. A variety of e-noses were recently assessed in clinical trials to diagnose SARS-CoV-2 infection: Nanose [13], Cyranose[®] [14-16], Aeonose [17], SpiroNose [18] and other developed electronic noses [19-21]. The characteristics of the related clinical trials are described in Table 1. To our knowledge, none of the previously presented e-noses was optimized to target specifically the VOC signature of a SARS-CoV-2 infection

identified by techniques discussed earlier. In this study, we aimed to optimize a sampling protocol and characterize the performance of Cyranose[®], a commercial e-nose, for the detection of common COVID-19-related VOC biomarkers in the breath.

2. Materials and Methods

2.1. Electronic nose

The commercial Cyranose 320 device (Sensigent[®], California, USA) was employed in the present study. This technology relies on a nanocomposite sensor array with 32 chemoresistive gas sensors for VOCs detection, where the electrical resistance of each sensor increases due to the adsorption of VOCs vapors on the sensors, exhibiting different sensitivities depending on polymers coated onto the individual sensor.

2.2. Vapors generation

The Cyranose[®] was characterized in the presence of vapor mixtures containing nitrogen, water vapor, acetone or nonanal. A gas bench mainly composed of valves, mass flow meters, permeation ovens and humidification columns was used to control various experimental parameters such as VOCs composition and concentrations, the relative humidity level and the gas flow rate. The analytical performances of Cyranose[®] were evaluated in the presence of VOC vapors injected continuously into glass cells during dynamic mode tests or by injecting known quantities of VOCs of interest into a Tedlar[®] bag during static mode tests. Thus, in dynamic mode tests, VOCs were prepared using permeation tubes containing standard analytical solution of acetone (99.8%, Carlo-Erba, France) or nonanal (95%, Sigma-Aldrich, France). Acetone and nonanal vapors were generated at low concentrations in the order of ppm to ppb levels following an additional dilution step with either dry or wet nitrogen.

Table 1. Clinical summary of key trials on the application of e-nose for SARS-CoV-2 diagnosis.

Year of Study	Country	E-nose	Type of sensors	Number of sensors	Number of patients	Reference
2020	Wuhan	Nanose	Gold nanoparticles + Organic ligands	8	140	[13]
2021	Mexico	Cyranose 320	Thin film carbon nanocomposite	32	84	[14]
2022	India				24	[15]
2022	Mexico				102	[16]

2020	Netherland	Aeonose	Metal oxide semiconductor (MOS)	3	219	[17]
2020	Netherland	Spirose	MOS	7	4510	[18]
2022	Thailand	A laboratory developed e-nose	MOS	8	17	[19]
2020	Italy	EOS507C	MOS	4	33	[20]
2021	Tel Aviv	PEN3 e-nose (AIRSENSE)	MOS	10	507	[21]

In static mode tests, a precise volume of acetone or nonanal was directly injected into a 3 Liter Tedlar[®] gas sampling bag (Thermogreen[®]) using a 2.5 μ L Syringe (Hamilton[®]). Additional components have been added to the experimental setup: a Labnet[®] mini-incubator was used to stabilize the temperature of the Tedlar[®] bags during static mode tests. Real-time measurements of the temperature and relative humidity of the gas flow were carried out using a Testo[®] 440 probe. Here acetone and nonanal concentrations were assessed using a ProCheck+ Photoionization detector (PID). The instrument is calibrated using isobutylene and a response factor was applied to provide direct readings of absolute values of acetone concentrations in nitrogen. For nonanal no response factor is available therefore we applied the response factor for TVOC as provided by the instrument's supplier, which we believe gives a good approximate of the nonanal concentration. The resulting concentrations measured were used in the calibration tests (Figure S1) and to estimate the concentrations of acetone and nonanal presented in Tables S1 and S2.

2.3. Evaluation of e-nose performance

All measurements carried out with the e-nose were preceded by a cleaning step, consisting in a dry N₂ purge for 60 minutes at the beginning of the day. In order to evaluate the Cyranose[®] response to both acetone and nonanal vapors and to determine the accuracy of the later quantification of both VOCs in exhaled breath, calibration tests were performed initially with these compounds in the dynamic mode. The resulting calibration curves are presented in Figure S1.

The next sections give the details of all experiments conducted to evaluate the e-nose performance in view of detecting the biomarkers of SARS-CoV-2 in the breath. For more clarity the list of experiments carried out is summarized in Table 2.

2.3.1. Sensitivity and stability of Cyranose[®] under humidified environments

Humidity is one of the main known parameter that can interfere with the response of the sensors. Thus, the sensors

responses to humidity variations were evaluated in dynamic sampling mode by varying the humidity levels from 16, 28, 40, 54, 66, 76 to 84%RH. The sampling process was performed with an average sampling rate of 120 mL/min, a sampling time of 90 seconds for both baseline and sample for six consecutive measurements.

In addition, the signal drift in the Cyranose[®] response was studied by evaluating the variance of the sensors response under humidified N₂ at 94%RH. This relative humidity value was chosen based on the relative humidity measured for exhaled breath filled in a Tedlar[®] bag, exhibiting a %RH value ranging from 92-94% RH. Tests were carried out during six consecutive cycles with ten measurements each. In these tests, a sampling time of 60 seconds was applied for dry N₂ (reference) and 90 seconds for N₂-94%RH.

2.3.2. Effect of sampling time and flow rate on sensor response

Developing an optimized analytical protocol is a priority for ensuring that breathing is analyzed under repeatable and reproducible conditions. Thus, tests were conducted in dynamic sampling mode to assess the influence of different experimental parameters on the sensitivity and stability of the Cyranose[®] sensors' responses: selection of an optimal sampling time for the analysis of exhaled breath is an important parameter to obtain a high quality of signal. Thus, the sensor's response was recorded during two exposures under N₂-94%RH, sampling at 50 mL/min, and by varying the exposure time from 35, 40, 50, 55 to 60 seconds.

In addition, the effect of varying sampling flow rate on the sensor response was evaluated under N₂-94%RH for ten repeat measurements of 20 seconds each and by varying the sampling flow rates, corresponding to the flow rates of the pump integrated into the e-nose: 50, 120 and 180 mL/min.

2.3.3. Exhaled breath analysis

Blank exhaled breath samples and exhaled breath samples spiked with acetone or nonanal were analyzed with the Cyranose[®]. For breath sample collection, the subject was asked not to eat, drink or smoke, nor to practice intensive exercise for three hours prior to collection. The donor

exhaled in a 3 Liter Tedlar[®] bag through a small Teflon tube, after remaining in a sitting position for 5 minutes. At this stage of the assessment, wash-in was not carried out prior to breath sample collection to minimize the effect of VOCs from the environments as suggested by Dragonieri and coworkers [22]. This is because the aim here was not to analyze VOCs exhaled from patients but rather assess whether the e-nose would be capable of detecting the presence of the addition of nonanal spiked in the breath sample. The first exhaled breath sample was directly analyzed as control. After waiting for 30 minutes without eating, drinking or smoking, the donor was asked for a second exhaled breath sample, which was then spiked with assessed (as described in Table S1&S2 in supplementary materials). For sample analysis using the e-nose, Cyranose[®] was operated at a constant flow rate of 120 mL/min for 60 seconds of baseline recording with ultra-pure nitrogen, and then for a sample-recording period of 90 seconds during ten repeat measurements. A sample stabilization and sensor re-activation procedure were also applied to the protocol: a dry N₂ purge step for 30 minutes was found helpful to reactivate

nonanal or acetone before analysis. Breath analysis was performed using the optimal experimental conditions previously described Table S3 summarizes all breath tests performed, also showing the Total Volatile Organic Compound (TVOC) concentrations measured by the PID at the end of each analysis.

In parallel, similar measurements using N₂-94%RH instead of breath samples were performed as a reference. For both types of experiments, a 3 Lite Tedlar[®] bag containing acetone (208ppb to 157ppm) or nonanal (TVOC varying from 817ppb to 53ppm) mixed with N₂-94%RH or exhaled breath was

the sensors and reduce noise in the signal reference. Also stabilization of sample temperature prior to analysis is important to avoid variability in VOCs composition. Consequently, samples were stabilized at 37°C (normal body temperature) for 5 minutes before each run.

Table 2 . Summary of the tests carried out to evaluate Cyranose[®] performance.

Experiments	Levels	Sampling process parameters	Repetitions
Sensitivity to humidity	<i>Humidity levels (%):</i> 16, 28, 40, 54, 66, 76 and 84.	Dynamic sampling mode. Baseline (dry N ₂) and sample (humidified N ₂), for both: - <i>Sampling flow:</i> 120 mL/min - <i>Sampling time:</i> 90 sec	One cycle per humidity level: six repeat measurements.
Stability under high humidity conditions	<i>Humidity level:</i> 94%RH	Static sampling mode: Tedlar [®] bag. Baseline (dry N ₂) and sample (humidified N ₂): - <i>Sampling flow:</i> 120 mL/min - <i>Sampling time:</i> 60 sec for baseline and 90 sec for sample	Six consecutive cycles: ten repeat measurements per cycle.
Effect of sampling time on sensor response to high humidity	<i>Exposure time (sec):</i> 35, 40, 50, 55 and 60.	Dynamic sampling mode. Baseline (dry N ₂) and sample (N ₂ -94%RH) - <i>Sampling time for baseline:</i> 60 sec - <i>Sampling flow:</i> 50 mL/min	One cycle per exposure time level: two repeat measurements.
Effect of flow rate on sensor response to high humidity	<i>Sampling flow (mL/min):</i> 50, 120 and 180.	Dynamic sampling mode. Baseline (dry N ₂) and sample (N ₂ -94%RH) <i>Sampling time: 60 sec for baseline and 20 sec for sample</i>	One cycle per sample flow level: ten repeat measurements.
Detection of Acetone in presence of exhaled breath	<i>Volume of acetone (µL):</i> 0, 0.5, 1, 1.5 and 2.5	Static sampling mode. One healthy donor. Baseline (N ₂ -94%RH) and sample (exhaled breath + acetone) - <i>Sampling time:</i> 60 sec for baseline and 90 sec for sample. - <i>Sampling flow:</i> 120 mL/min - <i>Sample temperature:</i> 37°C	One cycle per V(acetone): ten repeat measurements.

Detection of Acetone in humid nitrogen (reference)	Volume of acetone (μL): 0, 1 and 2.5	Static sampling mode. Baseline (N_2 -94%RH) and sample (acetone in N_2 -94%RH) - Sampling time: 60 sec for baseline and 90 sec for sample. - Sampling flow: 120 mL/min - Sample temperature: 37°C	One cycle per V(acetone): ten repeat measurements.
Detection of Nonanal in presence of exhaled breath	Volume of Nonanal (μL): 0, 0.5 and 1.5	Static sampling mode. One healthy donor. Baseline (N_2 -94%RH) and sample (exhaled breath + nonanal) - Sampling time: 60 sec for baseline and 90 sec for sample. - Sampling flow: 120 mL/min - Sample temperature: 37°C	One cycle per V(nonanal): ten repeat measurements.
Detection of Nonanal in humid nitrogen (reference)	Volume of Nonanal (μL): 0, 0.5 and 1.5	Static sampling mode. Baseline (N_2 -94%RH) and sample (nonanal in N_2 -94%RH) - Sampling time: 60 sec for baseline and 90 sec for sample. - Sampling flow: 120 mL/min - Sample temperature: 37°C	One cycle per nonanal V(nonanal): ten repeat measurements.

2.4. Data Processing

The electronic nose response was recorded in real-time by using the PC-nose software. A statistical data analysis was applied in order to discriminate between samples spiked or not with a VOC (nonanal or acetone). First, we calculate the increase in resistance of the 32 sensors according to Equation. 1:

$$\Delta R_s/R_0 = (R_s - R_0)/R_0, \quad (1)$$

Where R_s is the maximum resistance recorded for sensor s , and R_0 is the resistance of the same sensor obtained under ultra-pure nitrogen. Then we estimate the area under each of the 32 curves $\Delta R_s/R_0$ and use the Principal component analysis (PCA) to represent the initial data in a low dimension space. Finally, we apply a linear classifier (LDA) to build a decision linear boundary between the points of PCA plot representing the original exhaled breath samples and those spiked with a VOC (nonanal or acetone). Note that the chosen metric (area under the curve) does not intend to be generic, as the amount of data studied is relatively small. In other cases, this metric must be adapted to the type of electronic nose and the dynamics of its response to the measurement of exhaled air.

In this study, sample size estimation was not calculated, as all experiments were performed with exhaled breath from a single healthy volunteer.

The Cyranose[®] was firstly evaluated in the presence of dry acetone and nonanal vapors using permeation tubes filled with corresponding pure solutions. Experimental details are described in supplementary data. Calibration curves resulting for five sensors: S5, S6, S11, S23 and S31 that responded significantly, are presented in Figure S1. Based on the resulting linear equations, detection limit (LOD) for both VOCs, where $\text{LOD} = 3\sigma/\alpha$ (σ : standard deviation of the signal under dry nitrogen; α : slope of the linear equations) was calculated for sensor S31 to be 63ppb and 20ppb for acetone and nonanal, respectively.

The influence of humidity variation on the overall sensor array response is illustrated in Figure 1. Most Cyranose[®] sensors are not highly affected by various humidity changes, with the exception of five sensors (S5, S6, S11, S23 and S31) that exhibit a significant increase in resistance with the humidity increasing from 2% to 94%. This suggests that the detection of low concentrations of VOCs in exhaled breath may be strongly influenced by the presence of humidity.

An example of the signal recorded in dynamic sampling mode under humidified N_2 for six repeat measurements during exposure at 84%RH for sensor S31 is presented in Figure S2, exhibiting a stable sensor response with a calculated resistance variation of $3.5 \times 10^{-1} \pm 0.70\%$.

3. Results and Discussion

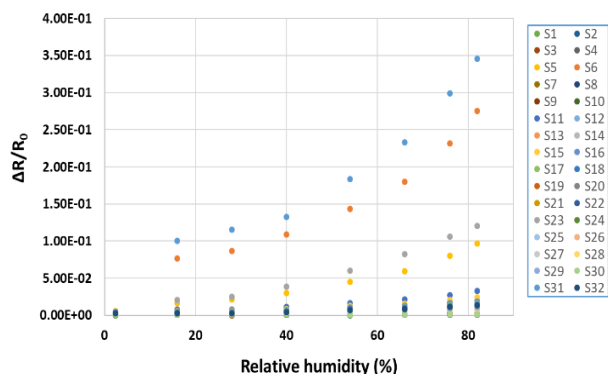


Figure 1. Resistance variations of 32 Cyranose® sensors during various RH changes.

Furthermore, the evaluation of the Cyranose® response under N_2 -94%RH during six exposure cycles (dry or wet), shows repeatable and stable resistance variations with no significant drift in signal as presented in Figure S3.

Setting an optimal sampling time for exhaled breath analysis is an important parameter to achieve a high quality of signal and to fix the time required for each exposure test. The response of S5 and S6 sensors resulting from two exposure tests under N_2 -94%RH at varying sampling time are shown in Figure 2. The results show a significant influence on the response of S6 for different sampling times, tending to a steady value starting from 60 seconds. On the contrary, sensors with smaller resistance variations under high humidity exposure such as S5, show a rapid saturation with water vapors at 35 seconds. Consequently, controlling the sampling time is a key parameter, which affects sensor resistance variation and thus the quality of the signal. As a result, a minimum sampling time of 60 seconds was found to be necessary to obtain a steady signal.

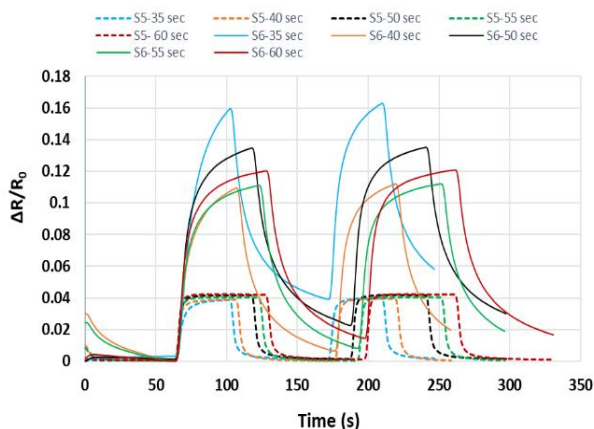


Figure 2. Real-time measurement of S5 and S6 sensors during two exposure tests under N_2 -94%RH at various sampling times: 35; 40; 50; 55 and 60 seconds.

Concerning the effect of sampling flow rate variation on sensor response to humidity from 0 to 94%RH, the majority

of Cyranose® sensors show negligible resistance variations upon flow rate changes, except for the five sensors S5, S6, S11, S23 and S31. An example is presented in Figure 3 in the case of sensor S31 during ten exposures at three sampling rate. A significant enhancement in sensor response to humidity was observed with increasing sampling flow rate from 50 mL/min to 180 mL/min. In this way, the interaction between water molecules and the Cyranose® sensor is more significant at a higher sampling flow rate. It can also be deduced that some of the sensors response depend indeed on the sampling flow rate applied. Therefore, an average flow rate of 120 mL/min was used as the optimal sampling flow rate in subsequent tests.

The ability of Cyranose® to detect low concentrations of acetone: a dominant VOCs in the exhaled breath, and nonanal: identified as one of COVID-19 biomarker, were evaluated both in exhaled breath from a healthy volunteer or in humidified nitrogen at 94%RH. Analysis of exhaled breath with Cyranose® was performed in a static sampling mode (described in paragraph 2.3.3), using the optimized experimental parameters (as detailed in Table 3). The results obtained were compared to the measurements using a sample matrix of N_2 -94%RH free of VOCs as reference.

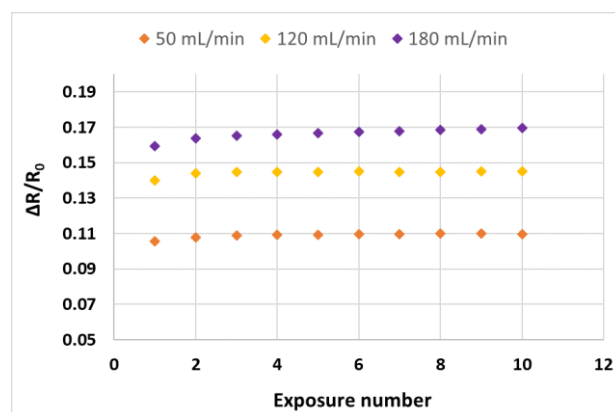


Figure 3. Resistance variations of S31 sensor for ten exposures under 94%RH at different sampling flow rate: 50, 120 and 180 mL/min.

PCA plots visualized in Figure 4 show a clear differentiation between the absence of acetone (**a1**) or nonanal (**b1**) in humidified nitrogen at 94%RH and after the injection of various volume of acetone (**a2**) or nonanal (**b2**) into the exhaled breath of the donor. Here concentrations of acetone and nonanal were ranging from 208ppb to 157ppm of acetone and from 25ppm to 75ppm of nonanal. The lowest concentrations of acetone and nonanal detected were 208ppb and 25ppm respectively. Additionally, the Cyranose® was able to differentiate between the different concentrations of acetone and nonanal injected. Although these concentrations are still high, in particular for nonanal which is more likely to be found at sub-ppm levels in the breath of COVID-19 patients, these results show that after sampling optimization

the device is able to detect the presence of these two volatile compounds in the breath with good reliability.

Table 3. Optimal experimental conditions used for the detection of acetone or nonanal traces in clean N₂-94%RH or breath samples for healthy volunteer.

Baseline Samples	Dry Nitrogen N ₂ -94%RH/ Exhaled Breath / Exhaled Breath-acetone/ Exhaled Breath-nonanal
Baseline purge (seconds)	60
Sample purge (seconds)	90
Sampling flow rate (mL/min)	120
Training repeat count	10
Measurement mode	Automatic
Sample temperature (°C)	37

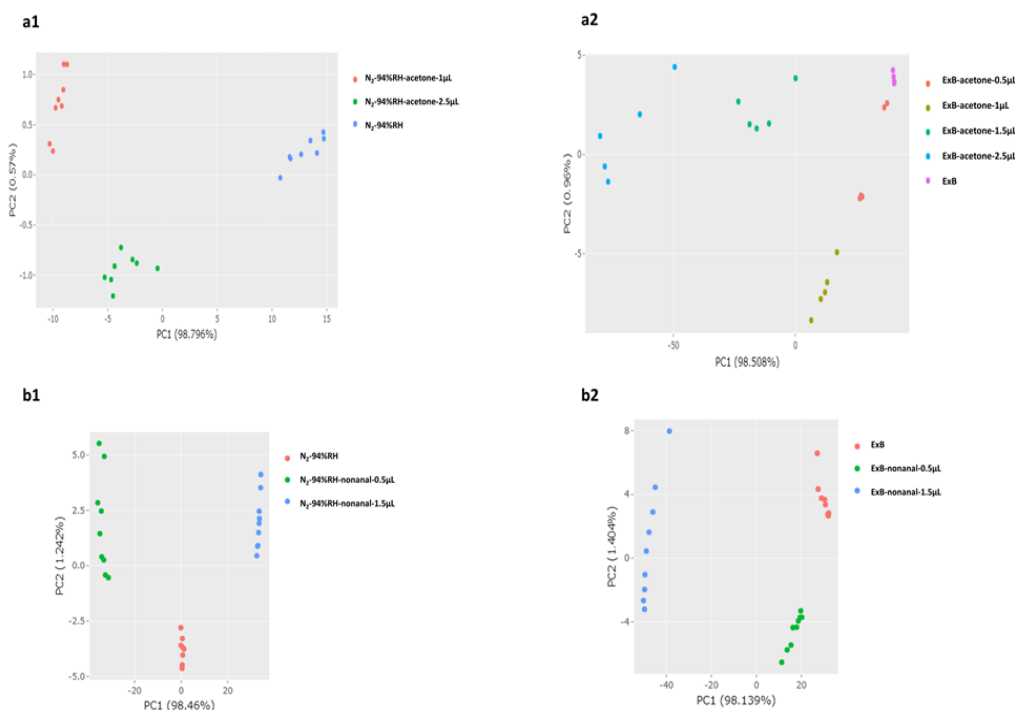


Figure 4. Component Analysis (PCA) plots of: **(a1)** acetone-N₂-94%RH; **(a2)** acetone-exhaled breath (ExB); **(b1)** nonanal-N₂-94%RH and **(b2)** nonanal-exhaled breath.

4. Conclusion

Aiming to optimize a protocol for identifying a specific respiratory imprint in COVID-19 patients based on an e-nose technology, a commercial electronic nose Cyranose[®] was characterized by evaluating the analytical performances in the presence of classic VOCs present in exhaled breath such as acetone and a putative biomarker of COVID-19: nonanal. The Cyranose[®] showed a stable and repeatable high sensor's sensitivity to relative humidity, which is normally present in

the breath. Additionally, Cyranose[®] sensor's response depends on various experimental parameters: temperature of the sampled air; sampling flow rate and sampling time. Thus, taking into account all these effects, an analytical protocol was optimized for breath analysis of healthy patients. Cyranose[®] revealed possible detection of low concentrations of acetone and nonanal injected into the exhaled breath of a healthy volunteer. Concentration as low as 25ppm of nonanal and acetone could be detected in breath samples in a reliable way. Further tests are now required to validate the possible

detection of the biomarkers at more realistic concentrations below the ppm range.

References

- [1] COVID-19 Map, Johns Hopkins Coronavirus Resource Center. (available at: <https://coronavirus.jhu.edu/map.html>) (Accessed 10 September 2022)
- [2] Shyu D, Dorroh J, Holtmeyer C, Ritter D, Upendran A, Kannan R, Dandachi D, Rojas-Moreno C, Whitt S P and Regunath H 2020 Laboratory Tests for COVID-19: A Review of Peer-Reviewed Publications and Implications for Clinical Use. *Mo. Med.* **117** 184–95
- [3] Ackermann M, Verleden S E, Kuehnel M, Haverich A, Welte T, Laenger F, Vanstapel A, Werlein C, Stark H, Tzankov A, Li W W, Li V W, Mentzer S J and Jonigk D 2020 Pulmonary Vascular Endothelialitis, Thrombosis, and Angiogenesis in Covid-19. *N. Engl. J. Med.* **383** 120–8
- [4] Lawal O, Ahmed W M, Nijsen T M E, Goodacre R and Fowler S J 2017 Exhaled breath analysis: a review of ‘breath-taking’ methods for off-line analysis *Metabolomics* **13** 1–16
- [5] Pajot-Augy É 2019 L’haleine et les capteurs d’odeurs *médecine/sciences* **35** 123–31
- [6] Mansour E, Vishinkin R, Rihet S, Saliba W, Fish F, Sarfati P and Haick H 2020 Measurement of temperature and relative humidity in exhaled breath *Sens Actuators B Chem* **304** 12737
- [7] Smith D, Španěl P, Herbig J and Beauchamp J 2014 Mass spectrometry for real-time quantitative breath analysis *J. Breath Res.* **8** 027101
- [8] Pleil J D and Lindstrom A B 1995 Measurement of volatile organic compounds in exhaled breath as collected in evacuated electropolished canisters *J. Of Chromatography B* **665** 271–279.
- [8] Grassin-Delyle S, Roquencourt C, Moine P, Saffroy G, Carn S, Heming N, Fleuriet J, Salvator H, Naline E, Couderc L J, Devillier P, Thévenot E A and Annane D 2021 Metabolomics of exhaled breath in critically ill COVID-19 patients: A pilot study *EBioMedicine* **63** 103154
- [9] Ruskiewicz D M, Sanders D, O’Brien R, Hempel F, Reed M J, Riepe A C, Bailie K, Brodrick E, Darnley K, Ellerkmann R, Mueller O, Skarysz A, Truss M, Wortelmann T, Yordanov S, Thomas C L P, Schaaf B and Eddleston M 2020 Diagnosis of COVID-19 by analysis of breath with gas chromatography-ion mobility spectrometry - a feasibility study *EClinicalMedicine* **29** 100609
- [10] Berna A Z, Akaho E H, Harris R M, Congdon M, Korn E, Neher S, M’Farrej M, Burns J and Odom John A R 2021 Reproducible Breath Metabolite Changes in Children with SARS-CoV-2 Infection *ACS Infect. Dis.* **7** 2596–603
- [11] Strike D J, Meijerink M G H and Koudelka-Hep M 1999 Electronic noses - A mini-review *Fresenius. J. Anal. Chem.* **364** 499–505
- [12] Gardner J W and Bartlett P N 1994 A brief history of electronic noses *Sensors Actuators B Chem.* **18** 210–1
- [13] Shan B, Broza Y Y, Li W, Wang Y, Wu S, Liu Z, Wang J, Gui S, Wang L, Zhang Z, Liu W, Zhou S, Jin W, Zhang Q, Hu D, Lin L, Zhang Q, Li W, Wang J, Liu H, Pan Y and Haick H 2020 Multiplexed Nanomaterial-Based Sensor Array for Detection of COVID-19 in Exhaled Breath *ACS Nano* **14** 12125–32
- [14] Rodríguez-Aguilar M, Díaz de León-Martínez L, Zamora-Mendoza B N, Comas-García A, Guerra Palomares S E, García-Sepúlveda C A, Alcántara-Quintana L E, Díaz-Barriga F and Flores-Ramírez R 2021 Comparative analysis of chemical breath-prints through olfactory technology for the discrimination between SARS-CoV-2 infected patients and controls *Clin. Chim. Acta* **519** 126–32
- [15] V. R. N, Mohapatra A K, V. K. U, Lukose J, Kartha V B and Chidangil S 2022 Post-COVID syndrome screening through breath analysis using electronic nose technology *Anal. Bioanal. Chem.* **414** 3617–24
- [16] Zamora-Mendoza B N, Díaz de León-Martínez L, Rodríguez-Aguilar M, Mizaikoff B and Flores-Ramírez R 2022 Chemometric analysis of the global pattern of volatile organic compounds in the exhaled breath of patients with COVID-19, post-COVID and healthy subjects. Proof of concept for post-COVID assessment *Talanta* **236** 122832
- [17] Wintjens A G W E, Hintzen K F H, Engelen S M E, Lubbers T, Savelkoul P H M, Wesseling G, van der Palen J A M and Bouvy N D 2021 Applying the electronic nose for pre-operative SARS-CoV-2 screening *Surg. Endosc.* **35** 6671–8
- [18] Slingers G, de Vries R, Vigeveno R M, Mulder S, Farzan N, Vintges D R, Goeman J J, Bruisten S, van den Corput B, Geelhoed M J J, Visser L G, van der Lubben M, Sterk P J, In T Veen J C C M and Groeneveld G H 2021 Ruling Out SARS-CoV-2 Infection Using Exhaled Breath Analysis by Electronic Nose in a Public Health Setting *TP91. TP091 EPIDEMIOLOGY AND TRANSLATIONAL ADVANCES IN SARS-COV-2* (American Thoracic Society) pp A3768–A3768
- [19] Phukkaphan N, Eamsa-Ard T, Aunsa-Ard W, Khunarak C, Nitivanichsakul T, Roongpuvapaht B and Kerdcharoen T 2022 Detection of COVID-19 infection based on electronic nose technique: preliminary study *International Electrical Engineering Congress (iEECON) (IEEE)* pp 1–4
- [20] Bax C, Robbiani S, Zannin E, Capelli L, Ratti C, Bonetti S, Novelli L, Raimondi F, Di Marco F and Dellacà R L 2022 An Experimental Apparatus for E-Nose Breath Analysis in Respiratory Failure Patients *Diagnostics* **12** 776
- [21] Snitz K, Andelman-Gur M, Pinchover L, Weissgross R, Weissbrod A, Mishor E, Zoller R, Linetsky V, Medhanie A, Shushan S, Jaffe E and Sobel N 2021 Proof of concept for real-time detection of SARS CoV-2 infection with an electronic nose *PLoS One* **16** 1–12
- [22] Dragonieri S, Quaranta V N, Carratù P, Ranieri T, Buonamico E and Carpagnano G E 2021 Breathing rhythm variations during wash-in do not influence exhaled volatile organic compound profile analyzed by an electronic nose *Molecules* **26** 2695